Atmospheric Pollution Research 16 (2025) 102504

Contents lists available at ScienceDirect

Atmospheric Pollution Research

journal homepage: www.elsevier.com/locate/apr

Integrated monitoring of road traffic and airborne ultrafine particles at a camera-equipped urban intersection

Tobias Schripp [a,1], Kay Gimm [b], Tobias Grein [a,*], Clemens Schicktanz [b], Stephan Weber [c], Markus Köhler [a]

[a] German Aerospace Center (DLR), Institute of Combustion Technology, Stuttgart, Germany
[b] German Aerospace Center (DLR), Institute of Transportation Systems, Braunschweig, Germany
[c] Technische Universität Braunschweig (TUBS), Climatology and Environmental Meteorology, Institute of Geoecology, Braunschweig, Germany

ARTICLE INFO

Keywords:
Mobile measurements
Non-volatile particles
Local air quality

ABSTRACT

This study investigated ultrafine particle concentrations at a busy intersection in Braunschweig, Germany, highlighting the influence of traffic as the primary source of elevated ultra-fine particle (UFP) concentrations. A mobile lab, equipped with online instruments for combustion gases and aerosols (SMPS, EEPS) was operated near to the intersection. By coupling a high-resolution particle size spectrometer with a catalytic stripper, it effectively characterized short-lived traffic-related particle events, outperforming traditional methods in resolving high-emission events. While total concentrations of particles with diameters between 4 nm and 3 µm were in the range of 6,000 #/cm^3 at low-traffic night hours, peak concentrations up to 3*10^6 #/cm^3 (10–20 s duration) could be observed under heavy traffic conditions. During daytime traffic, approximately 10 %–30 % of particles could not be evaporated at 350 °C. Traffic analysis was performed on a four-lane intersection equipped with 14 vertical stereo-camera-systems that allows a precise characterization of the traffic situation. While combining high-resolution particle measurements with a camera system showed potential for classifying transport modes, challenges such as limited differentiation between emission sources and complex data interpretation reduced its overall effectiveness compared to conventional methods.

1. Introduction

Air quality in cities has been a topic of high public interest for many years. In particular, the exposure to airborne particles is of great relevance (Kumar et al., 2014). The concentrations of inhalable particles (PM_{10}) are recorded at many measuring stations worldwide. The monitoring of particles that cannot be captured gravimetrically or direct optical methods is still incomplete though. For instance, the German "GUAN network" operates 16 stations that also record particle number concentrations of ultra-fine particles (UFP, diameter < 100 nm) (Sun et al., 2020). When detecting UFP, the attribution of the sources is a major challenge (Friend et al., 2012) due to several reasons. The spatial distribution of ultra-fine particles is highly variable due to moving sources (Birmili et al., 2013; Samad and Vogt, 2021), the high impact of meteorology (Giemsa et al., 2021; von Bismarck-Osten et al., 2013) and city topology (Duyzer et al., 2015). Furthermore, the aerosol ages and interacts with other airborne contaminants leading to changes in number, mass, size, volatility, and chemical composition (Jeong et al., 2015). However, a source apportionment can be achieved by clustering the data via positive matrix factorization (PMF). This has been successfully performed with PM_{10} (Beddows et al., 2015) and UFP (Kalkavouras et al., 2024) measurements.

One promising approach is the mobile monitoring of airborne particles in cities to gain information on their distribution (Alas et al., 2019). Numerous studies are published that used cars (Gerling and Weber, 2023; Tessum et al., 2018), bicycles (Ruths et al., 2014; Samad and Vogt, 2021), buses (Biondi et al., 2017), inner-city railways (Samad et al., 2021), full-equipped lab trucks (Drewnick et al., 2012; Ehlers, 2014; Kolb et al., 2004) or a carried out by foot (Liu et al., 2020). These studies showed that long-term monitoring of the same route is essential to get to conclusions on, e.g., influence of the engine type on emissions (Alas et al., 2019; Larson et al., 2017). Otherwise, mobile measurements only provide a phenomenological snapshot that is a superposition of meteorology (temperature, wind, rain, etc.), traffic situation and modes

* Corresponding author.
E-mail address: tobias.grein@dlr.de (T. Grein).
[1] now at: Zurich University of Applied Sciences (ZHAW), Center for Aviation, Winterthur, Switzerland

https://doi.org/10.1016/j.apr.2025.102504
Received 23 October 2024; Received in revised form 14 March 2025; Accepted 14 March 2025
Available online 19 March 2025

of transport. Many mobile measurements rely on small instruments and low-cost sensors. These are beneficial regarding power consumption and price but the correlation with research-grade aerosol instruments must be evaluated carefully (Asbach et al., 2018; Giordano et al., 2021). In particular, the differentiation between volatile and non-volatile particle fractions with low-cost sensors requires modified instruments that are preferably used for stationary measurements (Haugen et al., 2022).

Consequently, the full characterization of traffic-related aerosols requires sophisticated particle instruments and aerosol conditioning systems. Wehner et al. (2004) report measurements at two German highways using instruments for differentiating non-volatile and volatile airborne particles. They observed a higher non-volatile particle fraction in the size range 50–80 nm compared to a smaller particle mode (10–40 nm). Similar observations were reported by Birmili et al. (2010) during a 2-year observation in Augsburg (Germany). They report a reduction of up to 70 % in the original size of particles (60–200 nm) after passing through a thermal denuder at 300 °C. Traffic studies, thus, should cover particle number, mass, size, and volatility measurements to perform source related studies. They also require sophisticated and continuous monitoring of the local traffic conditions (number and type of vehicle), which, however, is usually not available at many study locations. Detailed traffic monitoring can be achieved by mobile camera modules (Knake-Langhorst and Gimm, 2016), roadside monitoring (Bishop et al., 2015) and other remote sensing techniques.

The present study demonstrates the potential of combining an advanced traffic monitoring system with lab-scale particle instruments to identify traffic-related emission sources and quantify their strength. First, mobile measurements were conducted in Braunschweig, Germany, to assess the representativeness of the DLR research intersection within the inner-city ring. This was followed by one week of stationary measurements, which were analyzed in conjunction with traffic data. Background measurements were also taken to account for potential biases from atmospheric processes.

2. Materials and methods

2.1. DLR mobile lab

The DLR mobile lab is based on a modified Volkswagen Crafter (Diesel engine), build up in 2020 by the team of the chemical analytics group from the DLR institute for combustion technology in Stuttgart.

A versatile infrastructure was installed in the loading space to allow flexible use for various experiments (Fig. 1). The core component is a frame made of aluminum grooved profiles, designed to hold measuring devices and auxiliary equipment, which are housed in custom-built boxes. The boxes are equipped with soft dampers between the inner and outer frame to prevent vibration artifacts during the mobile measurements. Since damping is most important for electrometer-based instruments that are highly sensitive to even low levels of vibration, the Engine Exhaust Particle Sizer is placed in its box via special wire rope mounts (Sebert Schwingungstechnik GmbH). The mobile laboratory features an independent IT system with LTE connectivity to the DLR network, enabling remote instrument access during stationary and mobile measurements. This proved vital during the COVID pandemic when driver and operator were in separate vehicles. It includes an external antenna, a GNSS positioning system (u-blox NEO-M9N) for precise tracking, and a roof-mounted air conditioning system maintaining 20–25 °C in the measurement section, supported by fans and temperature sensors. For stationary measurements, a weather station (Reinhardt MWS 55V) mounted 4 m above the vehicle records local atmospheric conditions. Power is supplied via three-phase current or optionally single-phase. For mobile use, a boost converter and 4000 Wh batteries, partially rechargeable by roof solar panels and the vehicle's alternator, are installed. For this study, the system was supplied by a nearby power box, which also supplied the servers for the camera system. Air sampling was performed via a roof inlet via conductive rubber tubing. The sampling flow was constant for mobile and stationary measurements.

2.2. AIM research intersection

The traffic data investigated was recorded at the Research Intersection operated by the German Aerospace Center (DLR). As part of the „Application Platform for Intelligent Mobility“ (AIM) (Knake-Langhorst et al., 2016), the Research Intersection is an urban multi-lane intersection at the inner-city ring road of Braunschweig with an average daily traffic intensity in the order of magnitude of approx. 35,000 vehicles during an average working day (Schicktanz et al., 2025). At the intersection, 14 vertical stereo-camera-systems are installed at different positions to cover the whole intersection and counteract occlusions of traffic participants. In 2021, the field of vision was extended into the arms to capture the behavior of traffic participants while they are entering and exiting the intersection. The mounted sensor setup allows the detection and classification of motorized and non-motorized traffic. In detail, a data processing pipeline fuses the camera data and the object detection results to output augmented videos and numerical trajectory data of all detected objects with a frequency of 25 Hz. The trajectory data consists not only of the positions but also of the velocity, acceleration, size, orientation and classification of the objects

Fig. 1. The DLR mobile lab for the measurement of particles and combustion gases. On the left side: View of the vehicle from the outside. On the right side: View of the mobile laboratory with built-in measuring devices.

(Knake-Langhorst and Gimm, 2016). In addition to the available camera sensors, two weather (PWD22, WXT530), two road (DSC211 and DST111), one solar radiation (SP Lite2) and one air quality sensor (AQT530) were installed at a pole at the south-east corner of the intersection at approx. 6 m height. A one-day example dataset from the AIM Research Intersection, showcasing the number of measured parameters, is publicly available (Schicktanz et al., 2025).

2.3. Mobile measurements

Mobile measurements were performed in Braunschweig from 03.08.2020 – 07.08.2020 during daytime. The general route followed the main streets of the inner two circles of the city and the surrounding high-speed roads in a free-roaming manner. Sampling was performed on the roof of the mobile lab at a height of approx. 3 m. The sampling rate was not adjusted to the wind speed (non-isokinetic sampling). A TSI 3752 Condensation Particle Counter (CPC) was used to measure the total particle number concentration (tPM_num) for particles >4 nm (D50) at a temporal resolution of 1 Hz. Since the sampling was not isokinetic, larger particles may be underrepresented. Even though the sampling situation was slightly more complex, the sampling efficiency for larger particles can be roughly estimated based on the sampling speed (4.9 m/s) and the wind speed (which was assumed to be the speed of the car) ranging from 50 to 100 km/h (Yoshida and Makino, 2006). The procedure was adopted from an experimental study on non-isokinetic sampling (Arouca et al., 2010). Under the given parameters, the sampling efficiency for particles with diameters <1 μm were above 90 %. The mobile lab recorded 16 h of data while driving 410 km in Braunschweig (6 h of data in the inner city). The exhaust pipe of the car is located mid car. The average daily temperature ranged from 16 °C (04.08.2020) to 24 °C (07.08.2020). No rain occurred during the week of measurement. The mobile measurements were accompanied by continuous background measurements (position B in Fig. 2) with a scanning mobility particle sizer using a unipolar charger (TSI 3910 NanoScan). The instrument measured the particle number size distribution from 11.5 nm to 365.2 nm in 13 channels at a 1 min interval.

2.4. Stationary measurements

The mobile lab was operated from 19.07.2021 – 24.07.2021 at a distance of approx. 50 m to the center of the intersection (Position A in Fig. 2). The lab was powered from a nearby power station to allow continuous operation of the instruments. A TSI 3752 CPC measured the total particle number concentration (tPM_num) in the range of 4 nm (D50) – 3 μm at 1 Hz (range: 0–10,000,000 #/cm^3; precision: ±5 % at < 100,000 #/cm^3 else ±20 %). A combination of a TSI Engine Exhaust Particle Sizer (EEPS) and a Catalytic Stripper (CS10, Catalytic Instruments) was used to monitor the non-volatile particle number concentration (nvPM_num) in the range of 5.6–560 nm. The EEPS determines the particle size distribution in 16 channels. The particle number concentration in each channel has been corrected for the losses in the catalytic stripper based on the penetration curve provided by the manufacturer. To compare the size distribution of the non-volatile and total particle fraction one Scanning Mobility Particle Sizer (SMPS, TSI 3082 Classifier, TSI 3776 CPC) was operated without pre-conditioning of the aerosol from July 20, 2021 12:00 to July 22, 2021 12:00. The SMPS measured the particle size distribution from 9 nm to 311 nm within 60 s (CPC range: 1,000,000 #/cm^3; CPC precision: ±10 % at < 300,000 #/cm^3). The SMPS was equipped with a diffusion dryer (TSI Modell 3062). The local carbon dioxide concentration was monitored via non-dispersive infrared spectroscopy by a LI-7200RS CO2/H2O Analyzer (LI-COR; range (CO_2): 0–3,000 ppm; precision: ±1 % of reading). Beside the MWS 55V, one additional weather station was operated at the opposite side of the street (position C in Fig. 2) near to the intersection at a traffic light pole (height approx. 5 m). The second weather station was to check the impact of the surrounding buildings on the wind situation at position A. Furthermore, another SMPS (TSI 3082 Classifier, TSI CPC 3752) was operated at a background measurement position (B in Fig. 2) at a distance of approx. 200 m to the intersection. The SMPS measured the particle size distribution from 11 nm to 359 nm within 60 s. The operation of the SMPS started one week prior to the installation of the mobile lab and was also operated one week after.

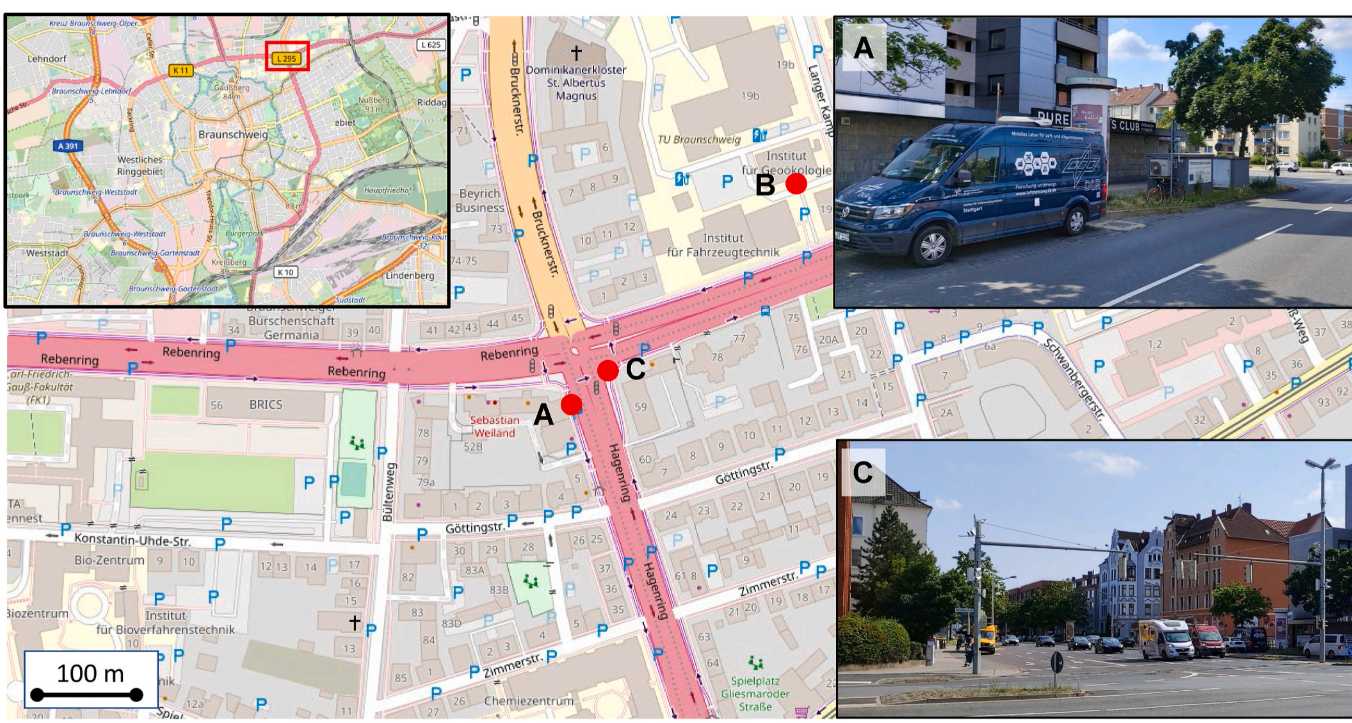

Fig. 2. AIM Research Intersection in Braunschweig, Germany. A: Sampling position of the mobile lab; B: "Background" measurement; C: Weather station at traffic light pole (Map: OpenStreetMap and contributors, CC-BY-SA).

3. Results and discussion

3.1. Citywide measurements

Braunschweig is a medium-sized German city with a population of approx. 250,000 (2020). The highest averaged traffic density can be found in the outer-ring streets which feature speed limits >50 km/h. Consequently, the highest particle number concentrations were observed here (Fig. 3, right). The box-plot (Fig. 3, left) summarizes the measured particle number concentrations during the mobile measurements, the vicinity of the intersection and the background measurements. The dots indicate the 95th and 5th percentiles, the whiskers mark the 90th and 10th percentiles, the box edges represent the 75th and 25th percentiles, and the line shows the median of the dataset. The inner-city particle number concentrations are near to the median concentration observed over the whole campaign (8,600 #/cm^3). The concentrations observed at the intersection (median 8,000 #/cm^3) are not significantly different than in the rest of the city (Fig. 3). The peak concentrations, however, are approx. 25 % lower (based on the 95th percentile). The background measurements have been performed at 200 m distance to the main streets (Position B in Fig. 2). Background concentrations (median: 5,780 #/cm^3) were lower than those from mobile measurements because the mobile sampling was conducted closer to the emission source. Furthermore, the lower cut-off diameter of the background monitoring (11.5 nm) was higher than the CPC used for the mobile measurements (D50 at 4 nm). This monitoring gap would lead to lower values for the background monitoring. Nevertheless, long-term averaged particle number size distributions in urban areas show a minor contribution (<5 %) of particles between 4 nm and 11 nm compared to the total particle number concentration (Birmili et al., 2010). Typical cars with combustion engines emit particles >20 nm depending on fuel and engine type. Vehicle chasing studies with sophisticated instruments showed that sub-10 nm particles can significantly contribute to the overall particle number concentration (Rönkkö et al., 2023). Since the majority of the sub-40-nm particles originating from traffic are volatile (Rönkkö et al., 2023), they will not reach the background monitoring unchanged. Due to this aerosol aging and differences in instrumentation, directly comparing the performed in-traffic measurements with background monitoring involves greater uncertainties.

Due to the high number of influencing parameters (weather, traffic density, traffic type, speed, etc.) the observed concentrations during the mobile measurements should not be used beyond the scope of this analysis. The data reveal that measurements at the intersection (red rectangle in Fig. 3) are comparable to the nearby main streets. This might be associated by the similar city topology, traffic composition and speed limits.

3.2. Ambient conditions during stationary measurements

The air temperature during stationary measurements near the intersection varied between 13 °C and 28 °C and the observation days showed similar pattern in temperature and relative humidity (Fig. 4). The maximum wind speed was 15.7 km/h while the median wind speed was 4 km/h. No rain occurred during the campaign. The wind direction at the measurement site was dominated by south-western wind (Fig. 5). As shown in Fig. 2, the mobile lab was stationed next to an eight-story building to the west. The wind directions recorded at the measurement site (A, Fig. 2) showed a reasonable correlation with those from the sensor array on the opposite street side (C, Fig. 2) for southwesterly winds (200°–250°). However, for easterly winds, position A appeared to be sheltered compared to position C. This discrepancy is likely due to the sensor array's more open location and closer proximity to the intersection (see Figure SI8 and SI9). In general, the wind directions aligned with the street corridors. Therefore, Weber et al. decided to differentiate between "along canyon" and "cross canyon" flow in a similar study in Essen, Germany (Weber et al., 2013). Based on the wind data at position A it was concluded that emissions from the intersection to the north did not significantly affect the roadside measurements and, thus, the data was not further differentiated. The measured concentrations primarily originated from vehicles traveling south past the measurement site and vehicles approaching the intersection. Consequently, the algorithm analysis of the recorded video data focused on this region.

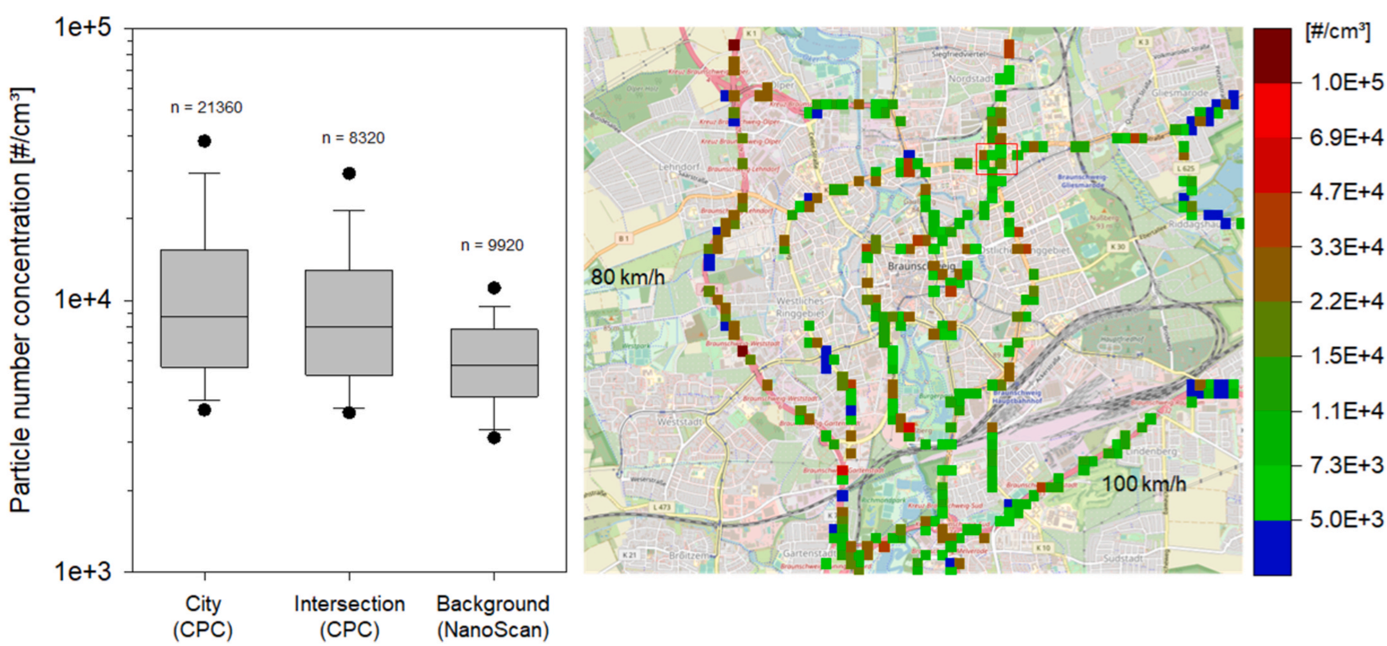

Fig. 3. Box-plot of the particle number concentrations (left) measured during mobile measurements in Braunschweig ("city"), in the vicinity of the AIM research intersection ("intersection", red rectangle) and the continuous background monitoring (position B in Fig. 2) in 2020. The map (right) shows the measured concentrations during the mobile measurements in a 100 m × 100 m grid. Grid points with <5 data points and a relative standard deviation > 50 % were discarded. Speed limits in the city are 30–50 km/h. Other speed limits are marked on the map (Map: OpenStreetMap and contributors, CC-BY-SA).

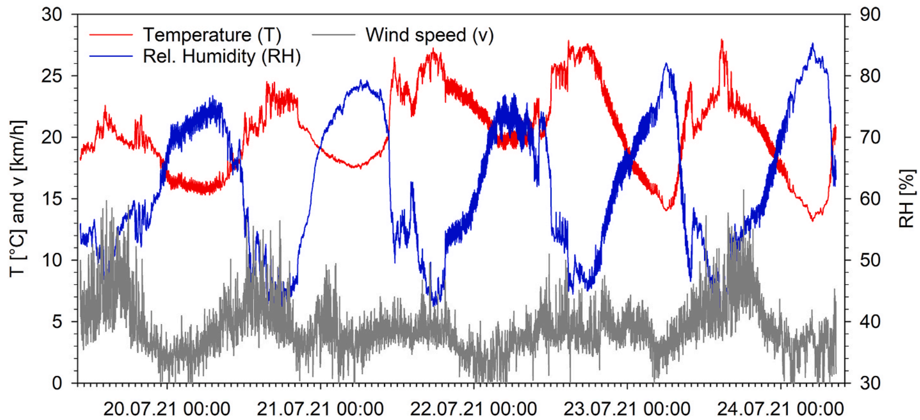

Fig. 4. Ambient temperature, relative humidity and wind speed at the measurement position and a time resolution of 1 min (A in Fig. 1).

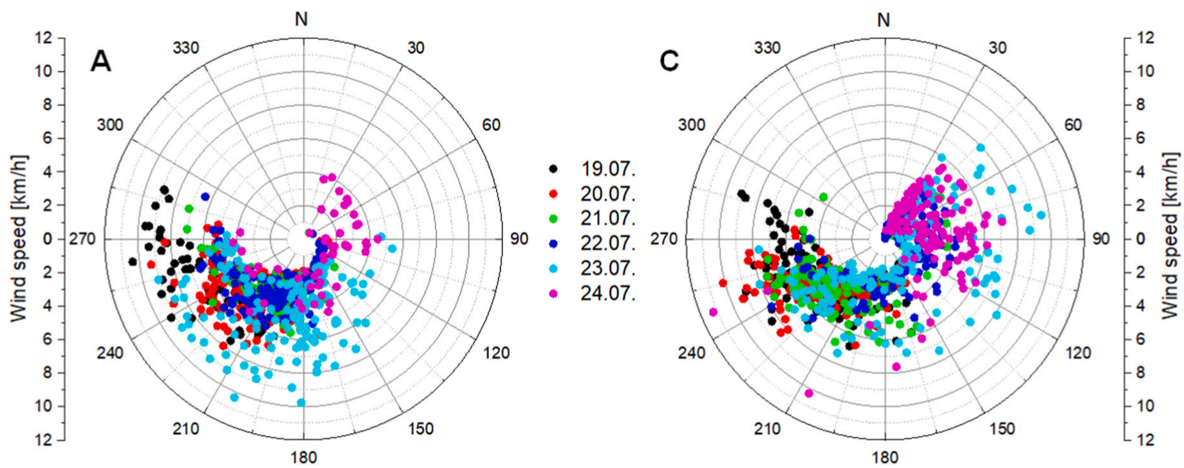

Fig. 5. Wind situation (10 min average) at the measurement site (A) and on the other side of the street (C) from Monday (19 07 2021) to Saturday (24 07 2021).

3.3. Background monitoring

Atmospheric processes, such as the formation of secondary organic aerosols (SOA), could bias the correlation analysis between total particle number concentration and non-volatile particle number concentration at the intersection. One precursor for the formation of SOA is ozone

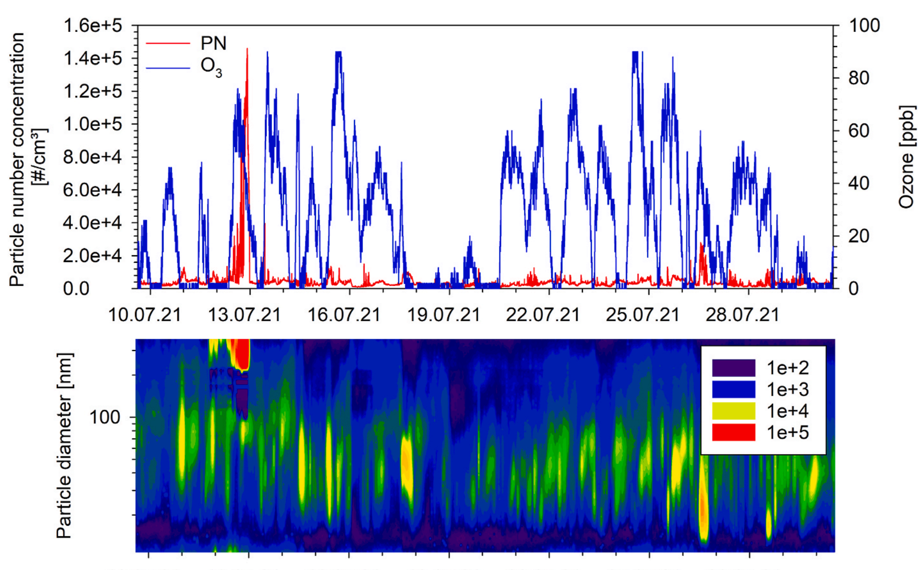

Fig. 6. Development of the particle number concentration (upper diagram) and particle size distribution (lower diagram) at the background measurement position (position B). The ozone concentration was monitored near the intersection (position C).

(Finlayson-Pitts and Pitts jr., 2000). Ambient ozone during the campaign showed a daily peak concentration of 60–80 ppb (Fig. 6). It must be noted though that the measurement was performed directly at the intersection. Elevated nitrogen oxide levels due to traffic are known to scavenge ozone. Therefore, the determination of the true ambient ozone levels is complicated in busy traffic areas (McConnell et al., 2006) and might lead to an underestimation. Nevertheless, it was expected that a formation of volatile particles was especially visible at the background measurement site due to less other sources. Two significant peaks in the particle number concentration were observed. The highest peak (12.07.) was caused by particles with diameter >200 nm (Figure SI4) which may be associated by a combustion source at distance. Another series of peaks on the 26.07. occurred in the afternoon hours. The particles mainly featured particle diameter below 100 nm (Figure SI7) and are mostly likely attributed to car movements nearby. Nevertheless, some smaller peaks on different days (Figure SI5 and SI6) showed a typical growth pattern for SOA formation (Heintzenberg et al., 2007). Furthermore, a photochemically induced particle formation event without subsequent particle growth likely occurred during the morning hours of 26.07. (Figure SI7). Since the above-mentioned events did not occur within the interval of the stationary monitoring at the intersection (19.07. – 24.07.) and the concentrations of the attributed SOA peaks were small compared to the concentrations at the intersection, we conclude that the stationary measurements were affected by background particle formation processes only to a minor extent.

3.4. Intersection monitoring

Throughout the campaign, the total number of airborne particles was consistently higher than the non-volatile particle fraction (Fig. 7). During the daytime, approximately 10 %–30 % of particles could not be removed by the catalytic stripper at 350 °C. This aligns well with previous studies in Aachen, which found that 10 %–20 % of traffic-related particles had a non-volatile core (Wehner et al., 2004). As expected, the non-volatile particle fraction increased with early morning traffic, starting around 5 a.m. On several days, a secondary increase in particle concentration was observed at night, beginning around 9 p.m., which did not align with traffic activity. This phenomenon is likely attributed to changes in the mixing layer height (MLH) during nighttime hours. Birmili et al. documented the influence of MLH on non-volatile particle volume concentrations in a long-term study conducted in Augsburg, highlighting a pronounced impact under winter conditions and a noticeable effect in summer (Birmili et al., 2010). Additionally, nearby sources, such as cooking or barbecues, may have contributed to this increase. Figure SI3 shows the development of the non-volatile particle size distribution in one night. Since after midnight a significant number of particles are sub-30 nm particles and the PSD remains stable, it is more likely that the atmospheric processes have a stronger impact than nearby sources. Overall, while airborne particle concentrations generally followed traffic patterns, a direct correlation was absent, likely due to the interplay of ambient conditions and variations in source strength.

It is important to note that the comparison involves instruments with different cut-off diameters. For the lower cut-off, the instruments are relatively similar (4 nm and 5.6 nm, respectively). However, the CPC's upper range is significantly higher than that of the EEPS. Despite this, the measured concentrations are largely influenced by traffic emissions. A comparison between CPC and SMPS data within the mobile lab shows minimal impact from particles >300 nm on a typical test day (Figure SI10). Given the strong correlation between CPC and SMPS (Figure SI11), a direct comparison with the CS + EEPS data is feasible.

The intraday analysis of the time-resolved particle monitoring reveals a very high number of particle number emission events (Fig. 8). The corresponding non-volatile particle size distributions mainly feature particles at a mode of 50 nm. This size is in good alignment with previous studies studying diesel exhaust with a sophisticated volatility measurement (Philippin et al., 2004). However, under free-flowing traffic conditions (e.g. around 12 a.m.) a second mode with sub-20 nm particles is detected. Similar observations have been reported in a field study in Aachen (Wehner et al., 2004). These particles may be attributed to soot emissions from passing vehicles, but also non-exhaust emissions could be a contributing factor. Overall, the median and peak (P95) particle number concentrations are in the same order of magnitude over the different weekdays (Table 1). This corresponds to a similar amount of traffic (Fig. 8). The maximum concentrations for each day represent very short-term particle events, e.g. plumes of passing vehicles, which could only be captured due to the high time-resolution of the instruments applied. The characterization of these short-term high emission events is not always possible based on the given data set.

A notable increase in non-volatile particle number concentration was observed for approximately 30 min before midnight on July 22 (Fig. 8). This rise is not accompanied by a substantial increase in carbon dioxide levels (Figure SI12). Additionally, the particle size distribution is very narrow, dominated by 10 nm particles. The source of this increase could potentially be a parked car in operation nearby or a smoker on the sidewalk, though neither can be detected by the monitoring system.

3.5. Characterization of single high emission events

The identification of single emission events is easy in low traffic conditions, e.g. during nighttime or early morning. In some cases, high

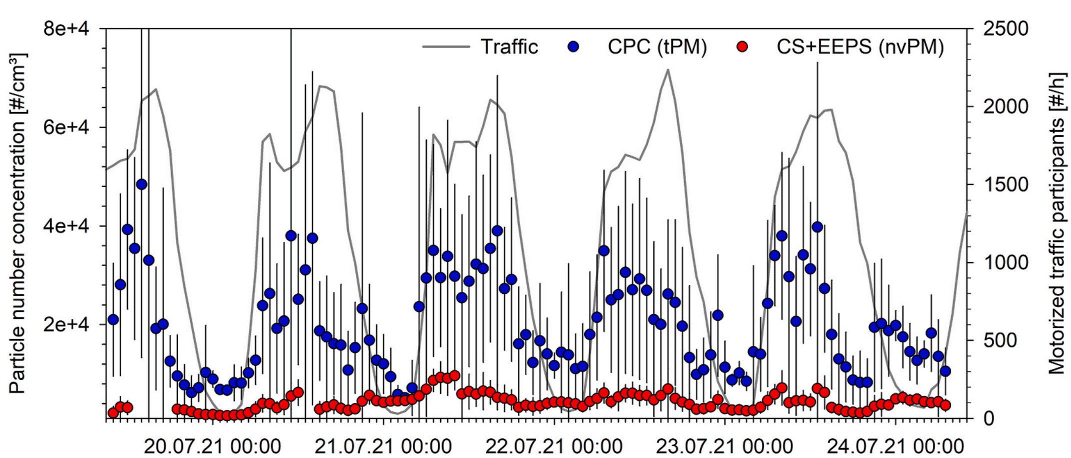

Fig. 7. 1 h-average particle number concentration recorded by a condensation particle counter (total fraction) and an Engine Exhaust Particle Sizer (EEPS) equipped with a catalytic stripper (CS, non-volatile fraction). The EEPS data was corrected for the loss in the CS. The number of motorized traffic participants was counted in the southern arm of the intersection.

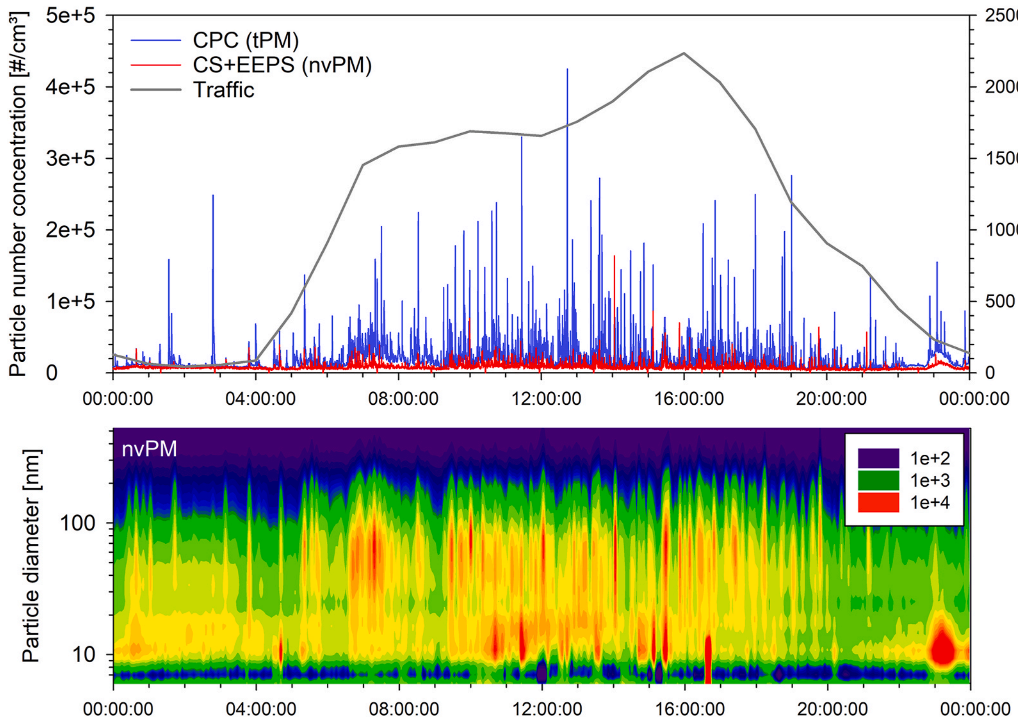

Fig. 8. Development of the particle number concentration (tPM, nvPM, 10 s average, upper diagram) and the non-volatile particle size distribution (2 min average, lower diagram) on the 22.07.21 at the intersection (position A).

Table 1
Particle number statistics (1 s time resolution) over the different weekdays monitored via condensation particle counter (CPC) and Engine Exhaust Particle Sizer equipped with catalytic stripper (CS + EEPS).

			tPM (CPC)				nvPM (CS + EEPS)			
Date	Weekday	Monitoring time	Min	Max	Median	P95	Min	Max	Median	P95
19 07 2021	Mo	10:00–23:59	5,761	571,502	21,960	52,750	2,136	106,022	4,221	14,272
20 07 2021	Tu	00:00–23:59	3,153	2,959,900	9,796	41,650	2,400	278,892	4,838	13,316
21 07 2021	We	00:00–23:59	3,586	1,196,498	17,495	58,808	1,782	158,073	7,332	19,783
22 07 2021	Th	00:00–23:59	3,981	856,224	12,830	52,068	1,276	402,902	7,386	16,199
23 07 2021	Fr	00:00–23:59	2,573	1,476,903	12,672	48,741	1,897	1,423,747	5,954	14,995

emission events could be narrowed to a limited number of vehicles even under regular traffic conditions. Fig. 9 shows a significant increase in the total and non-volatile particle number concentration. In contrast, the corresponding peak in carbon dioxide is less pronounced. This indicates a source with a high release of non-volatile particles in relation to the amount of fuel burnt. Several cars, one motorbike, and one truck passed the monitoring position. Some of these L-category vehicles (e.g. mopeds, motorcycles) feature high particle number emission factors during

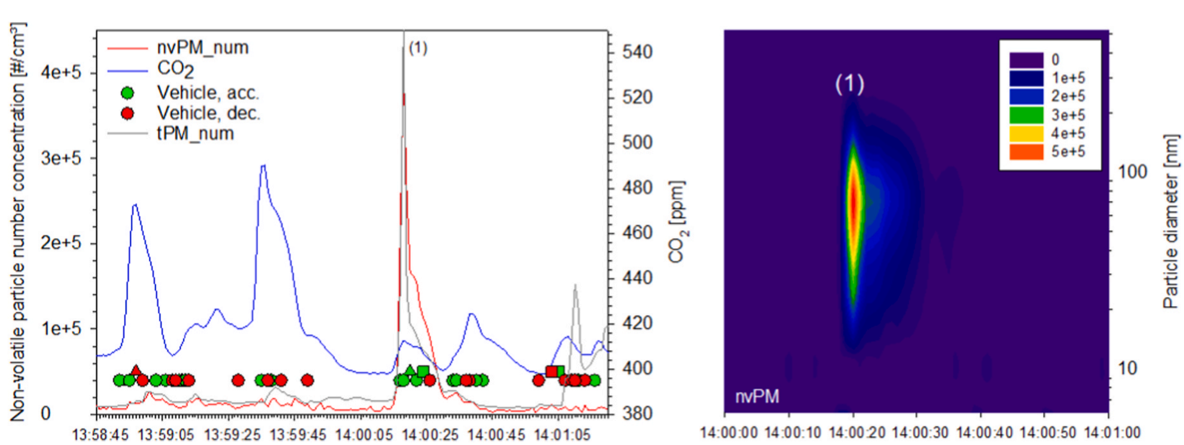

Fig. 9. Comparison of particle number concentration and carbon dioxide concentration on the 22 07 2021 (left diagram). The time events of vehicles in the southern arm of the intersection are marked in the diagram and distinguished by accelerating and decelerating vehicles (car: circle, triangle: motorbike, square: truck). The non-volatile size distribution of the peak event (1) is shown on the right side.

acceleration and the release of semi-volatile particles has been reported (Giechaskiel et al., 2019; Prati and Costagliola, 2009). The peak event (1) in Fig. 9 shows an increase in both, volatile and non-volatile particles. The non-volatile fraction shows a broad particle size distribution with a mode diameter of approx. 80 nm. The exact emission source cannot be determined due to mixing of the different plumes. Nevertheless, this example illustrates the complexity of source detection in the real environment and the attribution to traffic events. Before the high emission event (approx. at 13:59:00) several groups of vehicles passed the monitoring station without showing distinct peaks in the volatile or non-volatile particle number monitoring (Fig. 9). However, the mixed plumes are visible in the development of the carbon dioxide concentration. This trend can be also observed in the correlation between the different factors. While a general correlation between total and non-volatile particle number concentration can be observed (Figure SI1), the measured carbon dioxide concentration shows no proportional trend with the particle number concentration. High particle number concentrations for low carbon dioxide levels indicate the presence of exhaust plumes with very high particle load or the presence of other non-exhaust related emissions, such as brake and tire wear particles. These particles are formed from abrasion and feature mostly diameter above 100 nm (Bondorf et al., 2023) but also show nucleation particles in the 10 nm-range (Niemann et al., 2020) which feature a significant volatile fraction (Mamakos et al., 2021). Technically, the traffic monitoring system of the AIM intersection allows for the differentiation between accelerating and decelerating cars (Fig. 9). The reduction in speed is, however, not necessarily associated with mechanical brake usage. Therefore, a specific analysis for non-exhaust particle emissions cannot be performed from this data set. Further research is needed to determine whether an identification of the volatile non-exhaust particle fraction within the total particle number concentration is possible in environmental monitoring.

4. Conclusions

This study examined ultrafine particle concentrations at a busy traffic intersection and its vicinity in Braunschweig. The mobile measurements in this study demonstrated that traffic zones (e.g., inner city, city ring) can be differentiated to identify relevant measurement positions for background, hotspot, and average concentrations. However, they may not fully represent emissions near residential areas due to numerous changing influence factors. While many studies have investigated the number concentration and size distribution of ultrafine particles in the urban environment, the complexity of sources and processes often makes data interpretation challenging. This study demonstrated that coupling a high-resolution particle size spectrometer with a catalytic stripper can effectively resolve and characterize short-lived particle events linked to traffic (Fig. 9). This method outperforms a scanning particle size classifier in detecting point sources and high-emission events. Ideally, using two identical instruments with high temporal resolution for parallel measurements of total and non-volatile particle counts may provide the most accurate results. However, in this case, the total particle count was dominated by particles <300 nm. Thus, the tPM number concentration could be characterized by using a condensation particle counter. During the day, approximately 10–30 % of the particle number concentration could not be evaporated at 350 °C. The particles observed were primarily <100 nm in size, with some displaying bimodal distribution.

The high particle concentrations and small sizes indicate a nearby road as the primary source. This study also tested whether combining a comprehensive camera system with high-resolution particle measurement devices could help to classify different modes of transport. However, this approach faced several challenges. During the observation period, southerly winds prevailed, meaning the measurement location—south of the intersection—was primarily influenced by traffic on the road to and from the south. While the traffic data acquisition system enabled a focused analysis of this area, it could not adequately capture the overall complexity of the situation. Moreover, the purely optical recording and grouping of transport modes, without license plate recognition, lacked the ability to differentiate sufficiently between emission sources of different strength. Overall, this complex data collection system provided limited advantages over conventional traffic characterization methods. Nonetheless, it offered the capability to distinguish between accelerating and braking vehicles. Although this is of limited importance currently, it could become valuable for future air quality studies as electromobility grows and non-exhaust emissions gain significance.

CRediT authorship contribution statement

Tobias Schripp: Writing – review & editing, Writing – original draft, Data curation, Conceptualization. **Kay Gimm:** Writing – original draft, Supervision. **Tobias Grein:** Methodology, Investigation, Conceptualization. **Clemens Schicktanz:** Formal analysis, Data curation. **Stephan Weber:** Writing – review & editing, Writing – original draft, Methodology, Data curation. **Markus Köhler:** Writing – original draft, Supervision, Project administration.

Declaration of competing interest

The authors declare that they have no known competing financial interests or personal relationships that could have appeared to influence the work reported in this paper.

Acknowledgements

This work has been funded by the internal DLR project "Kooperative Fahrzeugintelligenz und mechatronisches Fahrwerk (NGC KoFiF)".

Appendix A. Supplementary data

Supplementary data to this article can be found online at https://doi.org/10.1016/j.apr.2025.102504.

References

Alas, H., Weinhold, K., Costabile, F., Di Ianni, A., Müller, T., Pfeifer, S., Di Liberto, L., Turner, J., Wiedensohler, A., 2019. Methodology for high-quality mobile measurement with focus on black carbon and particle mass concentrations. Atmos. Meas. Tech. 12, 4697–4712. https://doi.org/10.5194/amt-12-4697-2019.

Arouca, F., Feitosa, N., Coury, J., 2010. Effect of sampling in the evaluation of particle size distribution in nanoaerosols. Powder Technol. 200, 52–59. https://doi.org/10.1016/j.powtec.2010.02.007.

Asbach, C., Hellack, B., Schumacher, S., Bässler, M., Spreitzer, M., Pohl, T., Weber, K., Monz, C., Bieder, S., Schultze, T., Todea, A., 2018. Application possibilities and limitations of low-cost dust sensors. Gefahrst. Reinhalt. Luft 78, 242–250.

Beddows, D., Harrison, R., Green, D., Fuller, G., 2015. Receptor modelling of both particle composition and size distribution from a background site in London, UK. Atmos. Chem. Phys. 15, 10107–10125. https://doi.org/10.5194/acp-15-10107-2015.

Biondi, S., Catania, V., Monteleone, S., Polito, C., IEEE, 2017. Bus as a sensor: a mobile sensor nodes network for the air quality monitoring. Presented at the 13th International Conference on Wireless and Mobile Computing, Networking and Communications. IEEE WIMOB), pp. 272–277.

Birmili, W., Heinke, K., Pitz, M., Matschullat, J., Wiedensohler, A., Cyrys, J., Wichmann, H., Peters, A., 2010. Particle number size distributions in urban air before and after volatilisation. Atmos. Chem. Phys. 10, 4643–4660. https://doi.org/10.5194/acp-10-4643-2010.

Birmili, W., Rehn, J., Vogel, A., Boehlke, C., Weber, K., Rasch, F., 2013. Micro-scale variability of urban particle number and mass concentrations in Leipzig, Germany. Meteorol. Z. 22, 155–165. https://doi.org/10.1127/0941-2948/2013/0394.

Bishop, G., Hottor-Raguindin, R., Stedman, D., McClintock, P., Theobald, E., Johnson, J., Lee, D., Zietsman, J., Misra, C., 2015. On-road heavy-duty vehicle emissions monitoring system. Environ. Sci. Technol. 49, 1639–1645. https://doi.org/10.1021/es505534e.

Bondorf, L., Koehler, L., Grein, T., Epple, F., Philipps, F., Aigner, M., Schripp, T., 2023. Airborne brake wear emissions from a battery electric vehicle. Atmosphere 14. https://doi.org/10.3390/atmos14030488.

Drewnick, F., Böttger, T., von der Weiden-Reinmüller, S., Zorn, S., Klimach, T., Schneider, J., Borrmann, S., 2012. Design of a mobile aerosol research laboratory and data processing tools for effective stationary and mobile field measurements. Atmos. Meas. Tech. 5, 1443–1457. https://doi.org/10.5194/amt-5-1443-2012.

Duyzer, J., van den Hout, D., Zandveld, P., van Ratingen, S., 2015. Representativeness of air quality monitoring networks. Atmos. Environ. 104, 88–101. https://doi.org/10.1016/j.atmosenv.2014.12.067.

Ehlers, C., 2014. Mobile Messungen - Messung und Bewertung von Verkehrsemissionen, Schriften des Forschungszentrums Jülich. Köln.

Finlayson-Pitts, B.J., Pitts, jr J.N., 2000. Chemistry of the Upper and Lower Atmosphere - Theory, Experiments and Applications. Academic Press.

Friend, A., Ayoko, G., Jayaratne, E., Jamriska, M., Hopke, P., Morawska, L., 2012. Source apportionment of ultrafine and fine particle concentrations in Brisbane, Australia. Environ. Sci. Pollut. Control Ser. 19, 2942–2950. https://doi.org/10.1007/s11356-012-0803-6.

Gerling, L., Weber, S., 2023. Mobile measurements of atmospheric pollutant concentrations in the pollutant plume of BER airport. Atmos. Environ. 304. https://doi.org/10.1016/j.atmosenv.2023.119770.

Giechaskiel, B., Zardini, A., Lähde, T., Perujo, A., Kontses, A., Ntziachristos, L., 2019. Particulate emissions of euro 4 motorcycles and sampling considerations. Atmosphere 10. https://doi.org/10.3390/atmos10070421.

Giemsa, E., Soentgen, J., Kusch, T., Beck, C., Münkel, C., Cyrys, J., Pitz, M., 2021. Influence of local sources and meteorological parameters on the spatial and temporal distribution of ultrafine particles in Augsburg, Germany. Front. Environ. Sci. 8. https://doi.org/10.3389/fenvs.2020.609846.

Giordano, M., Malings, C., Pandis, S., Presto, A., McNeill, V., Westervelt, D., Beekmann, M., Subramanian, R., 2021. From low-cost sensors to high-quality data: a summary of challenges and best practices for effectively calibrating low-cost particulate matter mass sensors. J. Aerosol Sci. 158. https://doi.org/10.1016/j.jaerosci.2021.105833.

Haugen, M., Singh, A., Bousiotis, D., Pope, F., Boies, A., 2022. Differentiating semi-volatile and solid particle events using low-cost lung-deposited surface area and black carbon sensors. Atmosphere 13. https://doi.org/10.3390/atmos13050747.

Heintzenberg, J., Wehner, B., Birmili, W., 2007. "How to find bananas in the atmospheric aerosol": new approach for analyzing atmospheric nucleation and growth events. Tellus Ser. B Chem. Phys. Meteorol. 59, 273–282. https://doi.org/10.1111/j.1600-0889.2007.00249.x.

Jeong, C., Evans, G., Healy, R., Jadidian, P., Wentzell, J., Liggio, J., Brook, J., 2015. Rapid physical and chemical transformation of traffic-related atmospheric particles near a highway. Atmos. Pollut. Res. 6, 662–672. https://doi.org/10.5094/APR.2015.075.

Kalkavouras, P., Grivas, G., Stavroulas, I., Petrinoli, K., Bougiatioti, A., Liakakou, E., Gerasopoulos, E., Mihalopoulos, N., 2024. Source apportionment of fine and ultrafine particle number concentrations in a major city of the Eastern Mediterranean. Sci. Total Environ. 915. https://doi.org/10.1016/j.scitotenv.2024.170042.

Knake-Langhorst, S., Gimm, K., 2016. AIM Mobile Traffic Acquisition: instrument toolbox for detection and assessment of traffic behavior. JLSRF 2, A74. https://doi.org/10.17815/jlsrf-2-123.

Knake-Langhorst, S., Gimm, K., Frankiewicz, T., Köster, F., 2016. Test site AIM - toolbox and enabler for applied research and development in traffic and mobility. In: Rafalski, L., Zofka, A. (Eds.), Presented at the Transport Research Arena TRA2016, pp. 2197–2206. https://doi.org/10.1016/j.trpro.2016.05.235.

Kolb, C., Herndon, S., McManus, B., Shorter, J., Zahniser, M., Nelson, D., Jayne, J., Canagaratna, M., Worsnop, D., 2004. Mobile laboratory with rapid response instruments for real-time measurements of urban and regional trace gas and particulate distributions and emission source characteristics. Environ. Sci. Technol. 38, 5694–5703. https://doi.org/10.1021/es030718p.

Kumar, P., Morawska, L., Birmili, W., Paasonen, P., Hu, M., Kulmala, M., Harrison, R., Norford, L., Britter, R., 2014. Ultrafine particles in cities. Environ. Int. 66, 1–10. https://doi.org/10.1016/j.envint.2014.01.013.

Larson, T., Gould, T., Riley, E., Austin, E., Fintzi, J., Sheppard, L., Yost, M., Simpson, C., 2017. Ambient air quality measurements from a continuously moving mobile platform: estimation of area-wide, fuel-based, mobile source emission factors using absolute principal component scores. Atmos. Environ. 152, 201–211. https://doi.org/10.1016/j.atmosenv.2016.12.037.

Liu, X., Schnelle-Kreis, J., Zhang, X., Bendl, J., Khedr, M., Jakobi, G., Schloter-Hai, B., Hovorka, J., Zimmermann, R., 2020. Integration of air pollution data collected by mobile measurement to derive a preliminary spatiotemporal air pollution pro file from two neighboring German-Czech border villages. Sci. Total Environ. 722. https://doi.org/10.1016/j.scitotenv.2020.137632.

Mamakos, A., Kolbeck, K., Arndt, M., Schröder, T., Bernhard, M., 2021. Particle emissions and disc temperature profiles from a commercial brake system tested on a dynamometer under real-world cycles. Atmosphere 12. https://doi.org/10.3390/atmos12030377.

McConnell, R., Berhane, K., Yao, L., Lunnann, F., Avol, E., Peters, J., 2006. Predicting residential ozone deficits from nearby traffic. Sci. Total Environ. 363, 166–174. https://doi.org/10.1016/j.scitotenv.2005.06.028.

Niemann, H., Winner, H., Asbach, C., Kaminski, H., Frentz, G., Milczarek, R., 2020. Influence of disc temperature on ultrafine, fine, and coarse particle emissions of passenger car disc brakes with organic and inorganic pad binder materials. Atmosphere 11. https://doi.org/10.3390/atmos11101060.

Philippin, S., Wiedensohler, A., Stratmann, F., 2004. Measurements of non-volatile fractions of pollution aerosols with an eight-tube volatility tandem differential mobility analyzer (VTDMA-8). J. Aerosol Sci. 35, 185–203. https://doi.org/10.1016/j.jaerosci.2003.07.004.

Prati, M., Costagliola, M., 2009. Emissions of fine particles and organic compounds from mopeds. Environ. Eng. Sci. 26, 111–121. https://doi.org/10.1089/ees.2007.0206.

Rönkkö, T., Pirjola, L., Karjalainen, P., Simonen, P., Teinilä, K., Bloss, M., Salo, L., Datta, A., Lal, B., Hooda, R., Saarikoski, S., Timonen, H., 2023. Exhaust particle number and composition for diesel and gasoline passenger cars under transient driving conditions: real-world emissions down to 1.5 nm. Environ. Pollut. 338. https://doi.org/10.1016/j.envpol.2023.122645.

Ruths, M., von Bismarck-Osten, C., Weber, S., 2014. Measuring and modelling the local-scale spatio-temporal variation of urban particle number size distributions and black carbon. Atmos. Environ. 96, 37–49. https://doi.org/10.1016/j.atmosenv.2014.07.020.

Samad, A., Maali, A., Laquai, B., Vogt, U., 2021. Particulate matter profiles along the rack railway route using low-cost sensor. Atmosphere 12. https://doi.org/10.3390/atmos12020126.

Samad, A., Vogt, U., 2021. Spatial and temporal variability of NO2 and particulate matter concentrations along a busy federal highway in Stuttgart. Gefahrst. Reinhalt. Luft 81, 295–309.

Schicktanz, C., Klitzke, L., Gimm, K., Rizzo, G., Liesner, K., Mosebach, H.H., Knake-Langhorst, S., 2025. The DLR urban traffic dataset (DLR-UT): a comprehensive traffic dataset from the AIM research intersection. TechRxiv. https://doi.org/10.36227/techrxiv.174000540.08271707/v1.

Sun, J., Birmili, W., Hermann, M., Tuch, T., Weinhold, K., Merkel, M., Rasch, F., Müller, T., Schladitz, A., Bastian, S., Löschau, G., Cyrys, J., Gu, J., Flentje, H., Briel, B., Asbach, C., Kaminski, H., Ries, L., Sohmer, R., Gerwig, H., Wirtz, K., Meinhardt, F., Schwerin, A., Bath, O., Ma, N., Wiedensohler, A., 2020. Decreasing trends of particle number and black carbon mass concentrations at 16 observational sites in Germany from 2009 to 2018. Atmos. Chem. Phys. 20, 7049–7068. https://doi.org/10.5194/acp-20-7049-2020.

Tessum, M., Larson, T., Gould, T., Simpson, C., Yost, M., Vedal, S., 2018. Mobile and fixed-site measurements to identify spatial distributions of traffic-related pollution sources in los angeles. Environ. Sci. Technol. 52, 2844–2853. https://doi.org/10.1021/acs.est.7b04889.

von Bismarck-Osten, C., Birmili, W., Ketzel, M., Massling, A., Petäjä, T., Weber, S., 2013. Characterization of parameters influencing the spatio-temporal variability of urban particle number size distributions in four European cities. Atmos. Environ. 77, 415–429. https://doi.org/10.1016/j.atmosenv.2013.05.029.

Weber, S., Kordowski, K., Kuttler, W., 2013. Variability of particle number concentration and particle size dynamics in an urban street canyon under different meteorological conditions. Sci. Total Environ. 449, 102–114. https://doi.org/10.1016/j.scitotenv.2013.01.044.

Wehner, B., Philippin, S., Wiedensohler, A., Scheer, V., Vogt, R., 2004. Variability of non-volatile fractions of atmospheric aerosol particles with traffic influence. Atmos. Environ. 38, 6081–6090. https://doi.org/10.1016/j.atmosenv.2004.08.015.

Yoshida, H., Makino, H., 2006. Particle sampling in gas flow. In: Powder Technology Handbook. Third Edition, pp. 779–804. https://doi.org/10.1201/9781439831885-68.